Published in final edited form as:
Curr Biol. 2011 July 26; 21(14): 1239–1244. doi:10.1016/j.cub.2011.06.027.

Kinesin-3 KLP-6 regulates intraflagellar transport in male-specific cilia of *Caenorhabditis elegans*

Natalia S. Morsci[1,2] and **Maureen M. Barr**[1,*]

[1]Department of Genetics; Rutgers University; Piscataway, NJ 08854 USA

[2]Cell and Molecular Biology Program; University of Wisconsin – Madison; Madison, WI 53706 USA

Summary

Cilia are cellular sensory organelles whose integrity of structure and function are important to human health [1]. All cilia are assembled and maintained by kinesin-2 motors in a process termed intraflagellar transport (IFT), but exhibit great variety of morphology and function. This diversity is proposed to be conferred by cell-specific modulation of the core IFT by additional factors, but examples of such IFT modulators are limited [2–4]. Here we demonstrate that the cell-specific kinesin-3 KLP-6 acts as a modulator of both IFT dynamics and length in the cephalic male (CEM) cilia of *Caenorhabditis elegans*. Live imaging of GFP-tagged kinesins in CEM cilia showed partial uncoupling of the IFT motors of kinesin-2 family, kinesin-II and OSM-3/KIF17, with a portion of OSM-3 moving independently of IFT complex. KLP-6 moves independently of the kinesin-2 motors and acts to reduce the velocity of OSM-3 and IFT. Additionally, kinesin-II mutants display a novel CEM cilia elongation phenotype, which is partially dependent on OSM-3 and KLP-6. Our observations illustrate modulation of the general kinesin-2-driven IFT process by a cell-specific kinesin-3 in cilia of *C. elegans* male neurons.

Results

Intraflagellar transport (IFT) is the bidirectional movement of protein particles beneath the ciliary membrane between the tip and the base of the cilium [5]. IFT is essential for cilia formation and maintenance in mammals, nematodes, flies and ciliated protists [6–13]. In all cilia described to date, anterograde IFT is catalyzed exclusively by the kinesin-2 family motors. *Caenorhabditis elegans* amphid and phasmid sensory cilia are built by the cooperative action of two kinesin-2 motors: the kinesin-II heterotrimer (composed of the kinesins KLP-11/KIF3B, KLP-20/KIF3A and a kinesin-associated protein KAP-1) and the OSM-3/KIF17 homodimer [14]. Evidence of ciliogenic redundancy between these motors comes from the fact that either, but not both, is dispensable for IFT, although the degree of functional overlap varies between cilia type [2,14,15]. Cilia are morphologically diverse and functionally specialized. This specialization is proposed to be conferred by modulation of the core IFT by cell-specific factors [15], but examples of such IFT modulators are limited [2–4].

*Corresponding author: barr@biology.rutgers.edu Ph: (732) 445-1639 Fax: (732) 445-1147.

Kinesin-3 KLP-6 moves along CEM cilia independently of IFT motors

To study cell-type specific regulation of IFT, we focused on ciliated male-specific CEM neurons of *C. elegans*. In CEM cilia, kinesin-2 motors regulate levels of the TRP polycystin channel PKD-2/PC2 [16]. The CEMs also express an additional cilia-localizing kinesin-like protein 6 (KLP-6) [17], a conserved member of KIF28 subfamily of the kinesin-3 family of N-terminal kinesins (see Supplemental Experimental Procedures and [18]). KLP-6 is the only kinesin other than the kinesin-2 family known to regulate ciliary trafficking of PKD-2 [16,17]. Unlike the broad ciliated sensory neuron expression profile of kinesin-2 motors, *klp-6* is only expressed in a small subset of ciliated sensory neurons (IL2 and male-specific CEM, RnB, HOB), suggesting a role in specialization [17]. To determine whether KLP-6 is a motile kinesin, we visualized a GFP-tagged functional KLP-6 reporter in CEM cilia and measured its velocity by time-lapse fluorescence microscopy (Figure 1A1,2; Supplemental Movie 1, Figure S1A). KLP-6 moved at average velocity of ~0.7μm/s, and this velocity was not affected by the loss of either OSM-3 or KLP-11 (Figure 1B1, Table 1, Table S1). Rigor mutant KLP-6 reporter (S114N::GFP) did not move in the CEM cilia, indicating the functional requirement for ATP hydrolysis in KLP-6 motility (Figure 1A2,3 and Supplemental Movie 1). This data indicates that KLP-6 moves in CEM cilia, requires ATP and does not depend on kinesin-2 motors for its motility.

IFT motors kinesin-II and OSM-3 are partially uncoupled in CEM cilia

To characterize IFT in CEM cilia and measure the effect of KLP-6 on IFT dynamics, we recorded anterograde and retrograde ciliary movement of GFP-tagged functional reporters for IFT motors kinesin-II (KAP-1 subunit) and OSM-3 by time-lapse microscopy in wild-type and loss-of-function mutants *klp-11(tm324), osm-3(p802)* and *klp-6(my8)* (Figure 1B2,3; Table 1, Table S1, Supplemental Movies 2, 3). For experimental demonstration of functionality of all reporters, refer to Figure S1 and Figure S2A-C. IFT in CEM cilia is qualitatively different from amphid channel cilia, with considerably lower frequency of anterograde and retrograde movement events (compare kymographs in Figure 1 and Figure S1C2, Supplemental Movie 3). In wild-type CEM cilia, KAP-1::GFP moved at an average speed of ~0.5μm/s, while OSM-3::GFP traveled at significantly higher ~0.7μm/s average velocity (Table 1, Figure 1B2,3). This data indicates that a portion of OSM-3 motors is moving independently of kinesin-II as a separate, faster population in wild-type CEM cilia. However, the loss of the KLP-11 kinesin-II subunit resulted in increase of anterograde OSM-3 velocity from ~0.7 to ~0.9μm/s in *klp-11* mutants, suggesting that at least some OSM-3 motors are slowed down by kinesin-II in wild-type CEM cilia. The molecular mechanism of kinesin-II-mediated slowing of OSM-3 may be due to cooperative transport of the same IFT complexes, as occurs in amphid channel cilia [14]. We conclude that kinesin-2 motors are partially uncoupled in CEM cilia, with a mix of kinesin-II-OSM-3 complexes and OSM-3 alone. In kinesin-II-OSM-3 complexes, kinesin-II acts as negative regulator of OSM-3 velocity.

KLP-6 reduces the velocity of OSM-3 and KAP-1

The anterograde velocity of OSM-3::GFP increased from ~0.7 to ~0.9μm/s in *klp-6* mutants (Table 1, Figure 1B3), suggesting that OSM-3 is slowed down by KLP-6 in wild-type CEM cilia. The slowing effect of KLP-6 on OSM-3 persisted in *klp-11* mutants: the average OSM-3::GFP velocity increased from ~0.9μm/s in *klp-11* single mutants to ~1.1μm/s in *klp-6; klp-11* double mutants. Thus both KLP-6 and kinesin-II negatively regulate OSM-3 velocity, with inhibitory effects that are additive and independent.

The anterograde velocity of KAP-1::GFP increased from ~0.5 to ~0.7um/s in *klp-6* mutants, indicating that KLP-6 also slows down kinesin-II (Table 1, Figure 1B2). However, the inhibitory effect of KLP-6 was dependent on OSM-3, as KAP-1::GFP velocity decreased

from ~0.7um/s in the *klp-6* single to ~0.5 um/s in the *klp-6; osm-3* double mutants. Thus KLP-6 does not affect the velocity of KAP-1 directly, but rather indirectly through OSM-3 in kinesin-II-OSM-3 complexes. The significant difference in population velocities of OSM-3::GFP and KAP-1::GFP in *klp-6* mutants (~0.9 and ~0.7 um/s, respectively) indicates that despite an association with kinesin-II, a portion of OSM-3 is still moving as a separate, faster population. Our results suggest that KLP-6 acts to slow down OSM-3 and OSM-3/Kinesin-II motor complexes in CEM cilia.

IFT proteins are transported by the kinesin-II/OSM-3 motor complex

To understand basic IFT machinery in wild-type CEM cilia, we asked two questions: 1) Are IFT complex subunits A and B transported together? 2) What kinesins mediate their anterograde transport? We measured anterograde and retrograde movement of GFP-tagged functional reporters for IFT-A polypeptide CHE-11/IFT40, and IFT-B polypeptides OSM-5/IFT88 and OSM-6/IFT52 in CEM cilia of wild-type and various *klp-11, osm-3, klp-6* mutant combinations (Figure 1B4–6, Table 1, Table S1, Supplemental Movies 4,5)

The average anterograde velocity of IFT proteins ranged between 0.52–0.59 μm/s (Table 1). CHE-11::GFP (0.59 μm/s) was equal to OSM-5::GFP (0.57 μm/s), but slightly faster than OSM-6::GFP (0.52 μm/s), suggesting that CHE-11 and OSM-5 are transported together in wild-type CEM cilia. The average velocities of CHE-11, OSM-5 and OSM-6 in mutant cilia were comparable to KAP-1 when kinesin-II was present: 0.67–0.73um/s in *klp-6* single mutants and 0.44–0.48 um/s in *klp-6; osm-3* double mutants. The average velocities of CHE-11, OSM-5 and OSM-6 were comparable to OSM-3 when kinesin-II was absent: 0.91–1.06um/s in *klp-11* single mutants and 1.07–1.17um/s in *klp-6; klp-11* double mutants. Overall, CHE-11 had slightly higher average anterograde velocity but exhibited the same pattern of velocity changes as OSM-5 and OSM-6 in all the mutant genotypes (Figure 1B4–6). The data suggests that OSM-5, OSM-6 and CHE-11 are transported together as one complex in mutant CEM cilia.

We conclude that, in wild-type and *klp-6* CEM cilia, IFT-A-B complex is transported by the kinesin-II/OSM-3 motors, with minimal, if any, contribution from the faster OSM-3 motor alone. In the absence of kinesin-II, the IFT-A-B complex is transported by the OSM-3 motor alone. We conclude that the basic IFT machinery is similar between amphid channel and CEM cilia, and that the kinesin-3 KLP-6 acts at the level of the IFT kinesin-2 motors.

Kinesin-II is a negative regulator of CEM cilium length

Ciliary length is proposed to be modulated by transport in the cilium [19–21]. Hence we investigated how the loss of kinesin-II, OSM-3 and KLP-6 motors affect CEM cilium length using GFP-tagged βTubulin-4 as a marker of cilia axoneme (Figure 2, Fig S2C). Wild-type CEM cilia averaged at ~3.5±0.3μm in length and exhibited a stereotypic outward curve (Figure 2 B,J). The loss of KLP-11 resulted in abnormally long CEM cilia with an average of 5.1±.9μm (45% longer than wild-type) (Figure 2E,J). *klp-11* mutants also exhibited inwardly-curved CEM cilia, a phenotype previously reported by Bae *et al.* [16]. *kap-1(ok676)* and *klp-20(ok2914)* deletion mutants displayed similarly long and inwardly-curved CEM cilia (Figure S1 B3 and not shown), indicating that cilia elongation and inward curvature are kinesin-II loss-of-function phenotypes.

OSM-3 and KLP-6 mediate CEM cilium extension

The average length and shape of CEM cilia did not change in *osm-3* and *klp-6* single and double mutants (Figure 2C,D,G,J). The long cilia phenotype of *klp-11* mutants was partially dependent on the presence of KLP-6 and OSM-3, as the average CEM cilia length decreased to 4.6 ± 0.6μm in *klp-6; klp-11* double mutants and to 3.2 ± 1.1μm in *klp-11 osm-3* double

mutants (Figure 2J). The cilia-like projections of *klp-11 osm-3* double and *klp-6; klp-11 osm-3* triple mutants were highly variable in length, shape, orientation and exhibited large accumulations of tubulin at the cilia base (Figure 2F), illustrating the requirement of at least one IFT motor in CEM ciliogenesis. The CEMs of *klp-6; klp-11 osm-3* triple mutants showed either a complete loss of cilia or formation of very truncated (2.2±0.5μm) projections (Figure 2I,J). Overall, these results suggest that KLP-11 plays a restrictive role in determination of CEM cilia length; and that OSM-3 and KLP-6, although dispensable for determination of wild-type CEM cilia length, mediate its elongation.

We observed two main changes in IFT dynamics between wild-type and elongated CEM cilia: increased anterograde velocity and increased anterograde frequency of IFT events. The anterograde velocity and frequency of IFT polypeptides OSM-5, OSM-6, CHE-11 almost doubled in elongated cilia of *klp-6, klp-11* double mutants (Table 1, Mean and particles per cilium, PpN). At this point we cannot conclude whether either is the cause or the consequence of the increased cilia length. Retrograde velocity, although variable among reporters, did not differ significantly between wild-type and long cilia for any IFT polypeptide or kinesin (Table S1). We observed no correlation between frequency and velocity for any reporter within a given genotype and between changes in anterograde IFT velocity and CEM cilia length across the genotypes. Our data illustrate the complexity of CEM cilia length regulation and suggests factors other than velocity of IFT transport determine cilia length.

Discussion

Our results provide the first demonstration of the kinesin-3 motor KLP-6 moving in cilia, modulating the velocities of IFT and kinesin-2 motors, and acting as a positive regulator of cilia length extension. We propose a model for specialization of IFT in CEM cilia (Figure 3B). In wild-type CEM cilia, kinesin-II and OSM-3 are partially uncoupled, such that a portion of OSM-3 moves separately from kinesin-II and does not significantly contribute to motility of IFT complexes. The partially uncoupled movement of IFT kinesins has previously been described in the AWB amphid wing cilia of *C. elegans* [2]. This phenomenon distinguishes CEM and AWB from amphid channel cilia, where OSM-3 and kinesin-II move jointly in the cilia middle segment (Figure 3A) [14,22]. Male-enriched ciliary kinesin KLP-6 acts to slow down OSM-3 in CEM cilia by an unknown mechanism. Our conclusions of the slowing effect of KLP-6 on OSM-3 are based on genetics and *in vivo* velocities, and are not dependent on the direct physical interaction between the two motors. Hence, it will be important to test our model using *in vitro* motility and reconstitution experiments with purified recombinant *C. elegans* OSM-3 and KLP-6, as done for kinesin-2 [23,24]. OSM-3 is proposed to act as an accessory motor dispensable for ciliogenesis but modulating IFT pathway in AWC and AWB olfactory cilia of *C. elegans* [2,15]. Similarly, expression of a dominant-negative construct of KIF17, the mammalian homolog of OSM-3, blocked ciliary targeting of olfactory cyclic nucleotide-gated channels without affecting cilia formation in canine kidney cells [25]. We propose that, in CEM cilia, OSM-3 and KLP-6 act as accessory motors in transport of cilia-specific cargo.

With regard to CEM cilia length, kinesin-II acts as a negative regulator and OSM-3 and KLP-6 as positive regulators. These observations distinguish CEM cilia from amphid channel cilia, where disruption of the kinesin-II has no effect on cilia length and *osm-3* mutants display truncated distal segments; and from *Chlamydomonas* flagella, where disruption of the kinesin-II abrogates ciliogenesis [2,14,15,26,27]. Hence, our findings illustrate a novel role of kinesin-II in cilia length restriction.

Our work provides the first illustration of how the canonical IFT machinery, represented by kinesin-2 anterograde motors and present in all ciliated cells, can be modified in cell-specific manner by involvement of an additional ciliary motor of the kinesin-3 family.

Highlights

- Kinesin-3 motor KLP-6 translocates along CEM cilia independently of IFT motors
- IFT motors kinesin-II and OSM-3 are partially uncoupled in CEM cilia
- KLP-6 and KLP-11 independently reduce OSM-3 motor velocity
- Kinesin-II is required for restriction of CEM cilia length

Supplementary Material

Refer to Web version on PubMed Central for supplementary material.

Abbreviations and nomenclature

KLP-6	kinesin-like protein 6; member of the kinesin-3 family, KIF28 subfamily
OSM-3	osmotic avoidance abnormal 3; kinesin-2 family homodimeric motor
Kinesin II	heterotrimeric motor complex consisting of KLP-20, KLP-11 and KAP-1 (kinesin-associated protein 1)
KLP-20, KLP-11	kinesin-like proteins 20, 11; kinesin-2 family motors

Acknowledgments

We thank Douglas Braun for isolation and Erik Peden for outcrossing of the *klp-6(my8)* allele; Andrew Jauregui, Young-Kyung Bae and Robert O'Hagan for construction of TBB-4, OSM-5, KAP-1, OSM-6, and NPHP-4 reporters; the Barr laboratory for discussions and constructive criticism of this manuscript; Philip Anderson, Erik Dent, Thomas Martin, Ahna Skop, and John White (University of Wisconsin – Madison) for critical feedback on this project; Barth Grant (Rutgers University) for numerous plasmids; and the *Caenorhabditis* Genetics Center and National Bioresource Project for the Nematode for strains. This work was funded by the National Institutes of Health (R01DK059418 and R01DK074746).

References

1. Fliegauf M, Benzing T, Omran H. When cilia go bad: cilia defects and ciliopathies. Nat. Rev. Mol. Cell Biol. 2007; 11:880–893. [PubMed: 17955020]
2. Mukhopadhyay S, Lu Y, Qin H, Lanjuin A, Shaham S, Sengupta P. Distinct IFT mechanisms contribute to the generation of ciliary structural diversity in *C. elegans*. EMBO J. 2007; 12:2966–2980. [PubMed: 17510633]
3. Burghoorn J, Dekkers MP, Rademakers S, de Jong T, Willemsen R, Swoboda P, Jansen G. Dauer pheromone and G-protein signaling modulate the coordination of intraflagellar transport kinesin motor proteins in *C. elegans*. J. Cell. Sci. 2010; (Pt 12):2077–2084. [PubMed: 20501698]
4. Burghoorn J, Dekkers MP, Rademakers S, de Jong T, Willemsen R, Jansen G. Mutation of the MAP kinase DYF-5 affects docking and undocking of kinesin-2 motors and reduces their speed in the cilia of *Caenorhabditis elegans*. Proc. Natl. Acad. Sci. U. S. A. 2007; 17:7157–7162. [PubMed: 17420466]

5. Kozminski KG, Johnson KA, Forscher P, Rosenbaum JL. A motility in the eukaryotic flagellum unrelated to flagellar beating. Proc. Natl. Acad. Sci. U. S. A. 1993; 12:5519–5523. [PubMed: 8516294]
6. Pazour GJ, Dickert BL, Vucica Y, Seeley ES, Rosenbaum JL, Witman GB, Cole DG. *Chlamydomonas* IFT88 and its mouse homologue, polycystic kidney disease gene tg737, are required for assembly of cilia and flagella. J. Cell Biol. 2000; 3:709–718. [PubMed: 11062270]
7. Pazour GJ, Baker SA, Deane JA, Cole DG, Dickert BL, Rosenbaum JL, Witman GB, Besharse JC. The intraflagellar transport protein, IFT88, is essential for vertebrate photoreceptor assembly and maintenance. J. Cell Biol. 2002; 1:103–113. [PubMed: 11916979]
8. Perkins LA, Hedgecock EM, Thomson JN, Culotti JG. Mutant sensory cilia in the nematode *Caenorhabditis elegans*. Dev. Biol. 1986; 2:456–487. [PubMed: 2428682]
9. Cole DG, Diener DR, Himelblau AL, Beech PL, Fuster JC, Rosenbaum JL. *Chlamydomonas* kinesin-II-dependent intraflagellar transport (IFT): IFT particles contain proteins required for ciliary assembly in *Caenorhabditis elegans* sensory neurons. J. Cell Biol. 1998; 4:993–1008. [PubMed: 9585417]
10. Nonaka S, Tanaka Y, Okada Y, Takeda S, Harada A, Kanai Y, Kido M, Hirokawa N. Randomization of left-right asymmetry due to loss of nodal cilia generating leftward flow of extraembryonic fluid in mice lacking KIF3B motor protein. Cell. 1998; 6:829–837. [PubMed: 9865700]
11. Pedersen LB, Geimer S, Rosenbaum JL. Dissecting the molecular mechanisms of intraflagellar transport in *Chlamydomonas*. Curr. Biol. 2006; 5:450–459. [PubMed: 16527740]
12. Cao Y, Park A, Sun Z. Intraflagellar transport proteins are essential for cilia formation and for planar cell polarity. J. Am. Soc. Nephrol. 2010; 8:1326–1333. [PubMed: 20576807]
13. Han YG, Kwok BH, Kernan MJ. Intraflagellar transport is required in *Drosophila* to differentiate sensory cilia but not sperm. Curr. Biol. 2003; 19:1679–1686. [PubMed: 14521833]
14. Snow JJ, Ou G, Gunnarson AL, Walker MR, Zhou HM, Brust-Mascher I, Scholey JM. Two anterograde intraflagellar transport motors cooperate to build sensory cilia on *C. elegans* neurons. Nat. Cell Biol. 2004; 11:1109–1113. [PubMed: 15489852]
15. Evans JE, Snow JJ, Gunnarson AL, Ou G, Stahlberg H, McDonald KL, Scholey JM. Functional modulation of IFT kinesins extends the sensory repertoire of ciliated neurons in *Caenorhabditis elegans*. J. Cell Biol. 2006; 5:663–669. [PubMed: 16492809]
16. Bae YK, Qin H, Knobel KM, Hu J, Rosenbaum JL, Barr MM. General and cell-type specific mechanisms target TRPP2/PKD-2 to cilia. Development. 2006; 19:3859–3870. [PubMed: 16943275]
17. Peden EM, Barr MM. The KLP-6 kinesin is required for male mating behaviors and polycystin localization in *Caenorhabditis elegans*. Curr. Biol. 2005; 5:394–404. [PubMed: 15753033]
18. Miki H, Okada Y, Hirokawa N. Analysis of the kinesin superfamily: insights into structure and function. Trends Cell Biol. 2005; 9:467–476. [PubMed: 16084724]
19. Dentler W. Intraflagellar transport (IFT) during assembly and disassembly of *Chlamydomonas* flagella. J. Cell Biol. 2005; 4:649–659. [PubMed: 16103230]
20. Marshall WF, Rosenbaum JL. Intraflagellar transport balances continuous turnover of outer doublet microtubules: implications for flagellar length control. J. Cell Biol. 2001; 3:405–414. [PubMed: 11684707]
21. Pan J, Snell WJ. *Chlamydomonas* shortens its flagella by activating axonemal disassembly, stimulating IFT particle trafficking, and blocking anterograde cargo loading. Dev. Cell. 2005; 3:431–438. [PubMed: 16139231]
22. Ou G, Blacque OE, Snow JJ, Leroux MR, Scholey JM. Functional coordination of intraflagellar transport motors. Nature. 2005; 7050:583–587. [PubMed: 16049494]
23. Imanishi M, Endres NF, Gennerich A, Vale RD. Autoinhibition regulates the motility of the *C. elegans* intraflagellar transport motor OSM-3. J. Cell Biol. 2006; 7:931–937. [PubMed: 17000874]
24. Pan X, Ou G, Civelekoglu-Scholey G, Blacque OE, Endres NF, Tao L, Mogilner A, Leroux MR, Vale RD, Scholey JM. Mechanism of transport of IFT particles in *C. elegans* cilia by the concerted action of kinesin-II and OSM-3 motors. J. Cell Biol. 2006; 7:1035–1045. [PubMed: 17000880]

25. Jenkins PM, Hurd TW, Zhang L, McEwen DP, Brown RL, Margolis B, Verhey KJ, Martens JR. Ciliary targeting of olfactory CNG channels requires the CNGB1b subunit and the kinesin-2 motor protein, KIF17. Curr. Biol. 2006; 12:1211–1216. [PubMed: 16782012]

26. Huang B, Rifkin MR, Luck DJ. Temperature-sensitive mutations affecting flagellar assembly and function in *Chlamydomonas reinhardtii*. J. Cell Biol. 1977; 1:67–85. [PubMed: 830657]

27. Kozminski KG, Beech PL, Rosenbaum JL. The *Chlamydomonas* kinesin-like protein FLA10 is involved in motility associated with the flagellar membrane. J. Cell Biol. 1995; (6 Pt 1):1517–1527. [PubMed: 8522608]

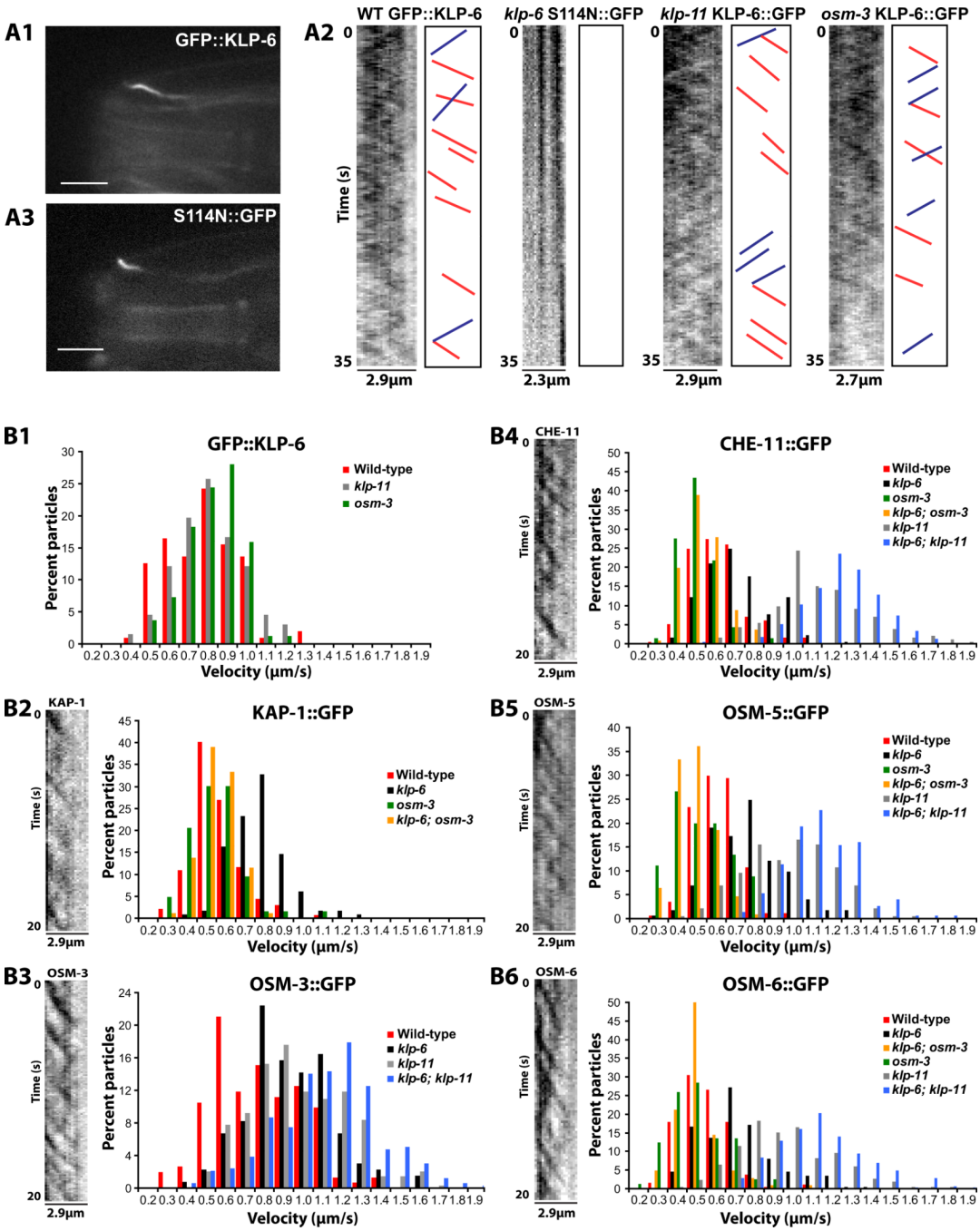

Figure 1. Velocity distribution of ciliary proteins in CEM cilia

(A1) Exemplary focal plane of GFP::KLP-6 in CEM cilium. Scale bar is 5µm. (A3) Exemplary focal plane of rigor KLP-6 reporter S114N::GFP in CEM cilium. Scale bar is 5µm. (A2) Inverted kymographs generated from time lapse stacks of GFP::KLP-6 in wild-type, *klp-11* and *osm-3* genetic backgrounds. Red and blue lines represent exemplary tracings used to measure anterograde and retrograde velocity, respectively. Rigor mutant KLP-6(S114N)::GFP shows no visible movement. Y=time, 35s, X=length of cilia trace. (B1) Histogram of GFP::KLP-6 particle motility in wild-type, *klp-11(tm324)* and *osm-3(p802)* CEM cilia. (B2-B6) Kymographs and velocity histrograms of particle motility of GFP-tagged KAP-1, OSM-3, CHE-11, OSM-5 and OSM-6 in CEM cilia. Y=time, 20s,

X=length of cilia trace. (B2) KAP-1::GFP particle motility. (B3) OSM-3::GFP particle motility. (B4) CHE-11::GFP particle motility. (B5) OSM-5::GFP particle motility. (B6) OSM-6::GFP particle motility. Genotypes are color coded and listed in the right corner of each histogram. Statistical analyses for (B-F) are shown in Table 1. Statistical analysis of particle velocity is shown in Table 1.

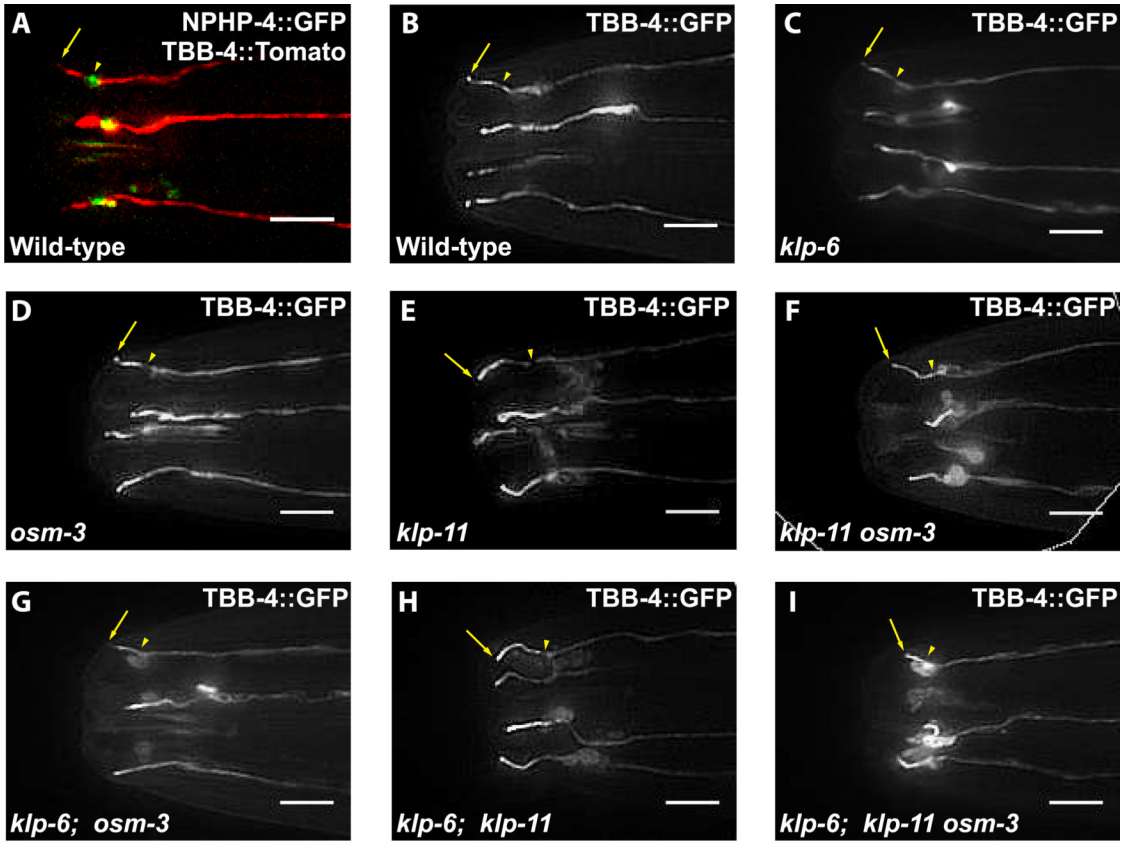

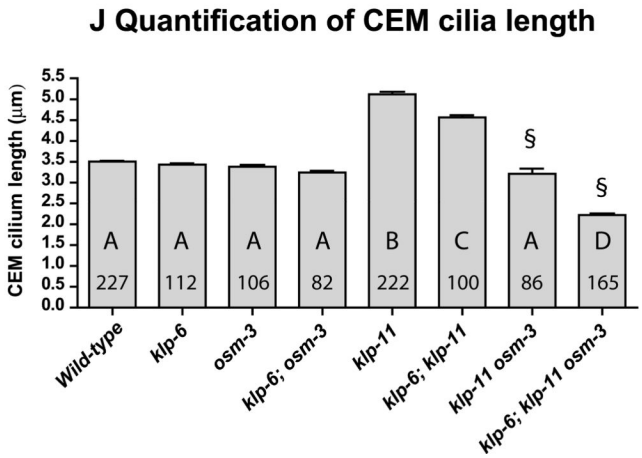

Figure 2. Effects of mutations in *klp-6* and IFT motors on CEM cilia morphology

(A) NPHP-4::GFP marks the transition zone (arrowhead) of CEM cilia labeled with TBB-4::tdTomato. The arrow points at the cilia tip. (B-I) Representative images of CEM cilia morphology labeled with TBB-4::GFP in (B) wild-type, (C) *klp-6*, (D) *osm-3*, (E) *klp-11*, (F) *klp-11 osm-3*, (G) *klp-6; osm-3*, (H) *klp-6; klp-11*, (I) *klp-6; klp-11 osm-3* animals. The scale bar is 5µm. To measure cilia length, we traced CEM cilia from the visible constriction at the transition zone (arrowhead) to the ciliary tip (arrow). (J) Bar graph of CEM cilia length averages. Each bar is the genotype mean ± standard error. The number within bars indicates the number of cilia scored; the letter indicates the results of statistical significance test. Genotypes sharing the same letter are not statistically different from each

other at $p<0.001$. § Cilia only measured, does not include animals with complete failure of CEM ciliogenesis.

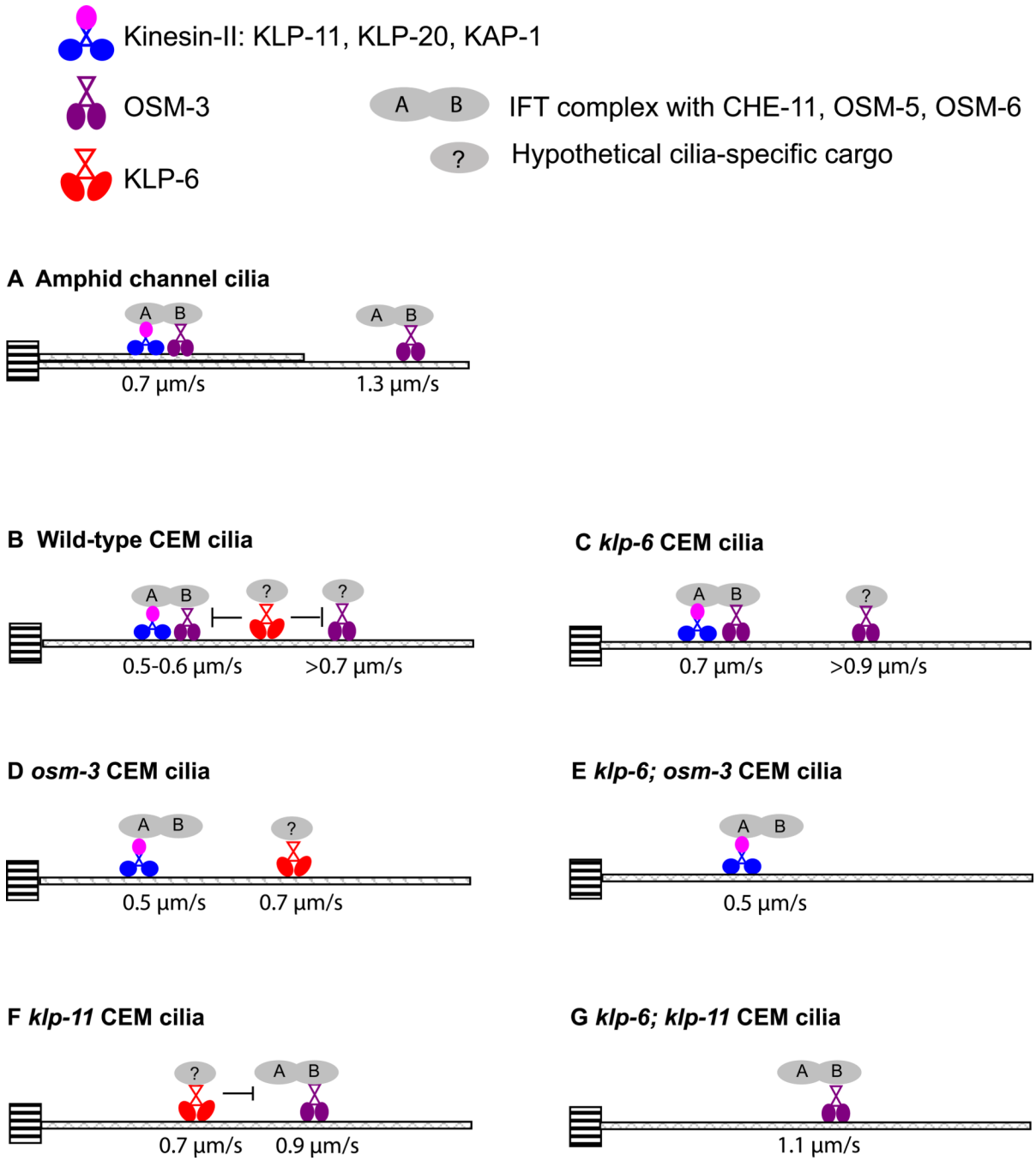

Figure 3. Specialization of intraflagellar transport

Diagrammatic representation of IFT in *C.elegans* (A) amphid channel cilia and (B-G) CEM cilia of different genotypes. The schematic model shows ciliary kinesins, their velocity and cargo. Kinesins are moving along the microtubule singlets or doublets that originate from the transition zone (indicated by striped box) and make up the ciliary axoneme. Kinesin-2 family is represented by heterotrimeric kinesin-II (KLP-11, KLP-20, KAP-1) and homodimeric OSM-3. Kinesin-3 family is represented by KLP-6. (A) Amphid channel cilia model, based on Snow et al. [14]. In the middle segment, defined by microtubule doublets, kinesin-II and OSM-3 cooperatively move the IFT complex at 0.7µm/s. In the distal segment, defined by microtubule singlets, OSM-3 alone moves IFT complex at 1.3µm/s. (B)

Male-specific CEM cilia. Kinesin-II and OSM-3 cooperatively move IFT complex. A subpopulation of fast OSM-3 motors does not contribute to mobilization of IFT, presumably due to recruitment by cell-specific cargo indicated by question mark. KLP-6 negatively regulates velocities of IFT and OSM-3. (C) In *klp-6* mutant CEM cilium, kinesin-II and OSM-3 motors cooperatively move IFT complex at 0.7μm/s; a sub-population of OSM-3 moves independently of IFT at a faster velocity. (D) In *osm-3* mutant CEM cilium, kinesin-II alone moves IFT complex. KLP-6 does not contribute to IFT movement. (E) In *klp-6 osm*-3 CEM cilium, kinesin-II alone moves IFT complex. (F) In *klp-11* CEM cilium, OSM-3 moves IFT complex at 0.9μm/s. KLP-6 moves at 0.7μm/s and retards OSM-3 mobility. (G) In *klp-11; klp-6* CEM cilium, OSM-3 moves IFT complex at 1.1μm/s.

Table 1

Velocity of anterograde transport in CEM cilia (μm/s)

	Ciliary kinesins											
	Kinesin-3				Kinesin-2							
	GFP::KLP-6				KAP-1::GFP				OSM-3::GFP			
Genotype	**Mean ± sd**	**n**	**N**	**PpN**	**Mean ± sd**	**n**	**N**	**PpN**	**Mean ± sd**	**n**	**K**	**PpN**
Wild type	0.72 ± 0.18[a]	103	16	6.4	0.52 ± 0.12[a]	137	34	4.0	0.73 ± 0.23[a]	152	18	8.4
osm-3	0.77 ± 0.14[a]	82	16	5.1	0.48 ± 0.14[a]	63	23	2.7	NA			
klp-6; osm-3	NA				0.49 ± 0.09[a]	87	25	3.5	NA			
klp-6	NA				0.73 ± 0.14[b]	116	29	4.0	0.89 ± 0.22[b]	134	12	11.2
klp-11	0.75 ± 0.17[a]	66	13	5.1	NA				0.92 ± 0.25[b]	347	30	11.6
klp-6; klp-11	NA				NA				1.07 ± 0.29[c]	335	26	12.9

	IFT polypeptides											
	IFT-A particle				IFT-B particle							
	CHE-11::GFP				OSM-5::GFP				OSM-6::GFP			
Genotype	**Mean ± sd**	**n**	**N**	**PpN**	**Mean ± sd**	**n**	**N**	**PpN**	**Mean ± sd**	**n**	**N**	**PpN**
Wild type	0.59 ± 0.14[a]	197	38	5.2	0.57 ± 0.11[a]	167	26	6.4	0.52 ± 0.13[a]	184	44	4.2
osm-3	0.45 ± 0.10[b]	69	23	3.0	0.48 ± 0.15[ab]	45	13	3.5	0.46 ± 0.15[a]	81	23	3.5
klp-6; osm-3	0.48 ± 0.10[b]	136	25	5.4	0.44 ± 0.10[b]	108	19	5.7	0.46 ± 0.11[a]	104	20	5.2
klp-6	0.67 ± 0.16[c]	181	25	7.2	0.73 ± 0.19[c]	173	22	7.9	0.68 ± 0.20[b]	198	32	6.2
klp-11	1.06 ± 0.25[d]	185	29	6.4	0.92 ± 0.23[d]	187	22	8.5	0.91 ± 0.27[c]	220	32	6.9
klp-6; klp-11	1.17 ± 0.19[e]	233	25	9.3	1.07 ± 0.19[e]	150	12	12.5	1.07 ± 0.23[d]	286	38	7.5

Indicated are mean anterograde velocities ± SD of GFP-tagged ciliary kinesins and IFT particle proteins. Values within a column followed by a common letter are not significantly different at $p<0.001$ based on one-way Anova with Bonferroni post-hoc test. n=number of particles traced, N=number of cilia imaged, PpN = particles per cilium, NA = not available. Anterograde velocity could not be measured in *klp-11 osm-3* double mutants due to severe ciliary abnormalities and large accumulations of reporters.